Gas Phase Synthesis of Triphenylene ($C_{18}H_{12}$)

Long Zhao,[a] Bo Xu,[b] Utuq Ablikim,[b] Wenchao Lu,[b] Musahid Ahmed,[b,*] Mikhail M. Evseev,[c] Eugene K. Bashkirov,[c] Valeriy N. Azyazov,[c,d] A. Hasan Howlader,[e] Stanislaw F. Wnuk,[e] Alexander M. Mebel,[c,e,*] Ralf I. Kaiser[a,*]

Abstract: For the last decades, the Hydrogen-Abstraction/ aCetylene-Addition (HACA) mechanism has been widely invoked to rationalize the high-temperature synthesis of PAHs as detected in carbonaceous meteorites (CM) and proposed to exist in the interstellar medium (ISM). By unravelling the chemistry of the 9-phenanthrenyl radical ($[C_{14}H_9]^•$) with vinylacetylene (C_4H_4), we present the first compelling evidence of a barrier-less pathway leading to a prototype tetracyclic PAH - triphenylene ($C_{18}H_{12}$) - via an unconventional Hydrogen Abstraction – Vinylacetylene Addition (HAVA) mechanism operational at temperatures as low as 10 K. The barrier-less, exoergic nature of the reaction reveals HAVA as a versatile reaction mechanism that may drive molecular mass growth processes to PAHs and even two dimensional, graphene-type nanostructures in cold environments in deep space thus leading to a better understanding of the carbon chemistry in our universe through the untangling of elementary reactions on the most fundamental level.

The 18-π aromatic triphenylene molecule ($C_{18}H_{12}$) has been at the center of attention in unraveling the underlying molecular mass growth processes leading to complex polycyclic aromatic hydrocarbons (PAHs) - organic molecules comprising fused benzene rings - on the most fundamental, microscopic level (Figure 1).[1] The ubiquitous presence of PAHs along with their alkylated counterparts in carbonaceous chondrites such as in Allende and Murchison suggests that PAHs may account for up to 20% of the cosmic carbon budget,[1-2] although most of them still remains unidentified.[3] Results from laser desorption – laser multiphoton ionization mass spectrometry (L^2MS) along with D/H and $^{13}C/^{12}C$ isotopic analyses of meteoritic PAHs reveal that meteoritic PAHs are not terrestrial contaminants, but rather have an extraterrestrial origin.[1, 4] Contemporary astrochemical models tackling the molecular growth processes to PAHs have been proposed to involve iron-based organometallic catalysis[5] or have been extrapolated from combustion chemistry reaction networks.[6]

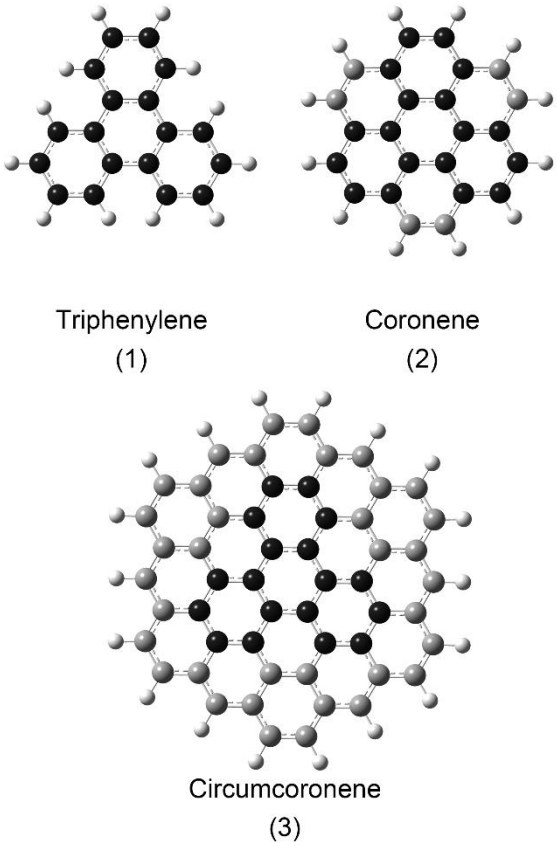

Figure 1. Molecular structures of triphenylene (1), coronene (2), and circumcoronene (3) highlighting the potential role of triphenylene as a key building block in the formation of graphene-type two dimensional nanostructures. The carbon atoms of the triphenylene building block are highlighted in black.

The popular Hydrogen-Abstraction/aCetylene-Addition (HACA) mechanism[7] has been remarkably prominent in making an effort to untangle the formation of PAHs in high temperature

[a] Dr. L. Zhao, Prof. Dr. R. I. Kaiser
Department of Chemistry
University of Hawaii at Manoa
Honolulu, Hawaii, 96822 (USA)
E-mail: ralfk@hawaii.edu
[b] Dr. B. Xu, Dr. U. Ablikim, Dr. Wenchao Lu, Dr. M. Ahmed
Chemical Sciences Division
Lawrence Berkeley National Laboratory
Berkeley, CA 94720 (USA)
E-mail: mahmed@lbl.gov
[c] Dr. M. M. Evseev, Prof. Dr. E. K. Bashkirov, Prof. Dr. V. N. Azyazov, Prof. Dr. A. M. Mebel
Samara National Research University
Samara 443086 (Russia)
E-mail: mebela@fiu.edu
[d] Prof. Dr. V. N. Azyazov
Department of Chemical & Electric Discharge Lasers
Lebedev Physical Institute of RAS
Samara 443011 (Russia)
[e] Dr. A. H. Howlader, Prof. Dr. S. F. Wnuk, Prof. Dr. A. M. Mebel
Department of Chemistry and Biochemistry
Florida International University
Miami, FL 33199 (USA)

Supporting information for this article is given via a link at the end of the document.

environments such as in combustion flames[6b-d] and in outflows of carbon-rich asymptotic giant branch (AGB) stars such as IRC+10216.[8] HACA involves a recurring sequence of atomic hydrogen abstractions from an aromatic hydrocarbon such as benzene followed by consecutive addition of one or two acetylene molecule(s) prior to cyclization and aromatization[8a, 8b, 9] with Parker et al. revealing that the three simplest PAHs carrying two, three, and four fused benzene rings - naphthalene ($C_{10}H_8$), phenanthrene ($C_{14}H_{10}$), and pyrene ($C_{16}H_{10}$) - can be synthesized at elevated temperatures via HACA-type mechanisms.[6b, 6d, 10] However, very recently, the ubiquity of the HACA concept was challenged when it was revealed that naphthalene can be synthesized via a *barrier-less* reaction at temperatures as low as 10 K involving the reaction of the phenyl radical ($[C_6H_5]^•$) with vinylacetylene (C_4H_4), the latter of which is supposed to be an important component in the atmosphere of large planets and interstellar medium,[11] through the hydrogen abstraction – vinylacetylene addition (HAVA) pathway.[6a, 12] However, despite its potential to synthesize PAHs in the cold interstellar medium, the legitimacy of HAVA to form PAHs beyond naphthalene has not been demonstrated experimentally, via molecular mass growth processes starting with aryl radicals and vinylacetylene.

In this *Communication*, by untangling the chemistry of the 9-phenanthrenyl radical ($[C_{14}H_9]^•$; 177 amu) with vinylacetylene (C_4H_4; 52 amu), we reveal the hitherto unknown chemistry synthesizing triphenylene ($C_{18}H_{12}$; 228 amu) - the prototype of a tetracyclic, benzenoid PAH composed only of benzene rings - along with atomic hydrogen (1 amu) (reaction (1)) via a de facto barrier-less HAVA reaction sequence. Briefly, a chemical reactor was utilized, products being detected isomer-specifically via fragment-free photoionization of the products in a molecular beam by tunable vacuum ultraviolet (VUV) time of flight mass spectrometry (Supporting Information).

(1) $[C_{14}H_9]^• + C_4H_4 \rightarrow C_{18}H_{12} + H^•$

An illustrative mass spectrum collected at a photoionization energy of 9.50 eV for the reaction of the 9-phenanthrenyl radical with vinylacetylene is portrayed in Figure 2a; reference spectra were also recorded by replacing the vinylacetylene reactant with non-reactive helium carrier gas (Figure 2b). These data deliver clear evidence on the synthesis of molecules with the molecular formulae $C_{16}H_{10}$ (202 amu) and $C_{18}H_{12}$ (228 amu) in the 9-phenanthrenyl – vinylacetylene system (Figure 2a), which are not present in the control experiment (Figure 2b). The $C_{18}H_{12}$ isomer(s) and atomic hydrogen is formed via reaction (1) of 9-phenanthrenyl with vinylacetylene while signal connected with $C_{16}H_{10}$ might be linked to the reaction of 9-phenanthrenyl with acetylene (C_2H_2; 26 amu) (Supporting Information, Fig. S1). Finally, ion counts at mass-to-charge ratios (*m/z*) of 259 ($C_{13}{}^{13}CH_9{}^{81}Br^+$), 258 ($C_{14}H_9{}^{81}Br^+$), 257 ($C_{13}{}^{13}CH_9{}^{79}Br^+$), 256 ($C_{14}H_9{}^{79}Br^+$), 179 ($C_{13}{}^{13}CH_{10}^+$), 178 ($C_{14}H_{10}^+$), 177($C_{14}H_9^+$/ $C_{14}{}^{13}CH_8^+$), and 176 ($C_{14}H_8^+$) are detectable in both the 9-phenanthrenyl - vinylacetylene and the 9-phenanthrenyl - helium systems. Therefore, these species are not associated with the reaction between 9-phenanthrenyl and vinylacetylene. Signal at *m/z* = 259 to 256 can be linked with the non-pyrolyzed 9-bromophenanthrene precursor; signal at *m/z* = 178 and 179 is attributed to phenanthrene and ^{13}C-phenanthrene formed via hydrogen abstraction by or hydrogen addition to the 9-phenanthrenyl radical; finally, ion counts at *m/z* = 176 and 177 are connected to phenanthryne isomers (*m/z* = 176) together with the 9-phenanthrenyl radical ($[C_{14}H_9]^{•+}$; *m/z* = 177) (Supporting Information, Fig. S1).

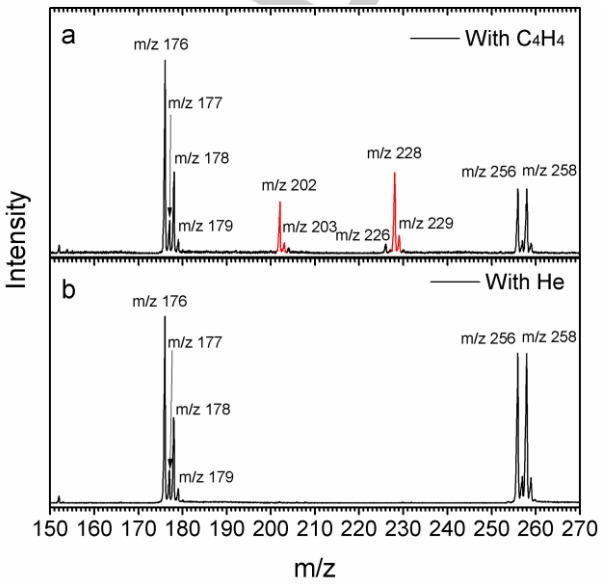

Figure 2. Comparison of photoionization mass spectra recorded at a photoionization energy of 9.50 eV for the (a) 9-phenanthrenyl ($[C_{14}H_9]^•$) - vinylacetylene (C_4H_4) and (b) 9-phenanthrenyl ($[C_{14}H_9]^•$) - helium (He) systems. The mass peaks of the newly formed $C_{16}H_{10}$ (*m/z* = 202) and $C_{18}H_{12}$ (*m/z* = 228) species along with the ^{13}C-substituted species (*m/z* = 203 and 229) are highlighted in red.

Our objective is to assign the structural isomer(s) of $C_{18}H_{12}$ synthesized in the elementary reaction of 9-phenanthrenyl with vinylacetylene, This requires a detailed analysis of the corresponding photoionization efficiency (PIE) curve, which illustrates the intensity of the ion at *m/z* of 228 ($C_{18}H_{12}^+$) as a function of the photon energy from 7.30 eV to 10.00 eV (Figure 3a). These data are fit with established reference PIE curves for distinct $C_{18}H_{12}$ isomers (triphenylene, chrysene, benz(a)anthracene, benzo(c)phenanthrene, 9-(but-3-en-1-yn-1-yl)-phenanthrene and (*E*)-9-(but-1-en-3-yn-1-yl)-phenanthrene (Supporting Information, Fig. S2). Here, the experimentally derived PIE curve at *m/z* of 228 (black) can be effectively replicated by the reference PIE curves ($C_{18}H_{12}^+$) of three isomers including triphenylene, 9-(but-3-en-1-yn-1-yl)-phenanthrene and (*E*)-9-(but-1-en-3-yn-1-yl)-phenanthrene. The experimental PIE curve reveals an onset of the ion signal at 7.60 ± 0.05 eV; this onset compares favorably with the adiabatic ionization energy of 9-(but-3-en-1-yn-1-yl)-phenanthrene at 7.60 ± 0.05 eV measured in this work. It should be noted that the PIE curve for *m/z* = 229 (Figure 3b) is, after scaling, superimposable on the PIE curve of *m/z* = 228. Therefore, the PIE function of *m/z* = 229 can be associated with the ^{13}C substituted isomers ($C_{17}{}^{13}CH_{12}$) of triphenylene, 9-(but-3-en-1-yn-1-yl)-phenanthrene and (*E*)-9-(but-1-en-3-yn-1-yl)-phenanthrene ($C_{18}H_{12}$). It is crucial to emphasize that the PIE curves of $C_{18}H_{12}$ isomers of triphenylene

are *characteristically associated* to each molecule highlighting that the co-existence of other isomers in the molecular beam would change the shape of the PIE significantly and hence can be excluded. Therefore, we determine that within our error limits, triphenylene, 9-(but-3-en-1-yn-1-yl)-phenanthrene and (*E*)-9-(but-1-en-3-yn-1-yl)-phenanthrene signify the contribution to signal at *m/z* of 228 and 229. Two sources add to the errors: ± 10% based on the accuracy of the photodiode and a 1 σ error of the PIE curve averaged over the individual scans.

The present work reveals that the prototype of a benzenoid PAH composed of four benzene rings – triphenylene – can be synthesized via the elementary reaction of the 9-phenanthrenyl radical with vinylacetylene. To untangle the underlying mechanism of formation, we performed electronic structure calculations on the relevant $C_{18}H_{12}$ and $C_{18}H_{13}$ potential energy surfaces (PESs) (Figure 4, Supporting Information, Fig. S3). Our computations reveal an overall barrier-less pathway leading to triphenylene at temperatures as low as 10 K found in cold molecular clouds in interstellar space. Here, the formation of triphenylene is initiated by the barrier-less formation of weakly bound van-der-Waals complexes of 9-phenanthrenyl and vinylacetylene **[1]** and **[6]**, in which the radical center of 9-phenanthrenyl points to the vinyl and ethynyl moieties of the vinylacetylene reactant, respectively.

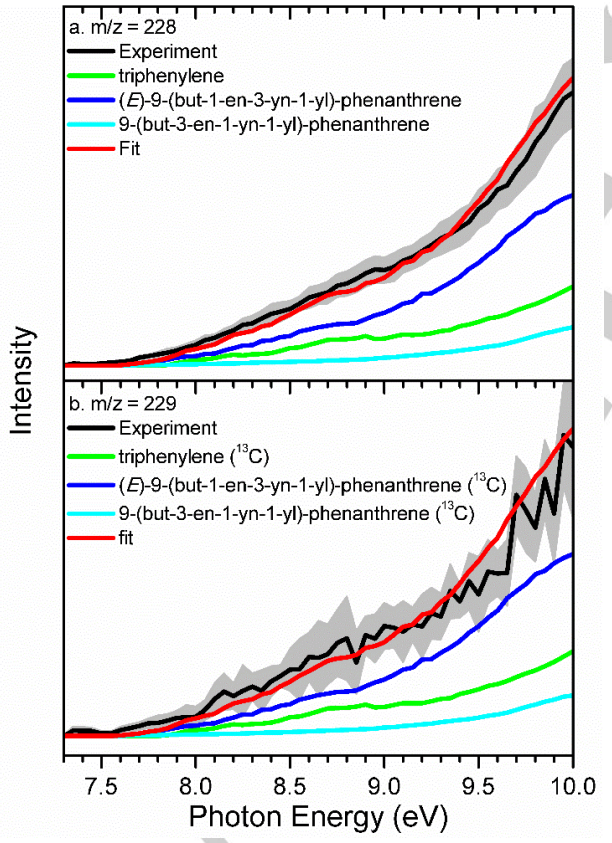

Figure 3. Photoionization efficiency (PIE) curves for *m/z* = 228 and 229. Black: experimentally derived PIE curves; Colored lines: reference PIE curves for triphenylene (green), (*E*)-9-(but-1-en-3-yn-1-yl)-phenanthrene (blue) and 9-(but-3-en-1-yn-1-yl)-phenanthrene (cyan), red: overall fit. The overall error bars consist of two parts: ±10% based on the accuracy of the photodiode and a 1 σ error of the PIE curve averaged over the individual scans.

The complex **[1]** can isomerize via addition of the radical center to the H_2C moiety of the vinylacetylene molecule through a barrier of only 5 kJ mol^{-1} leading to a resonantly stabilized free radical intermediate **[2]**, which is stabilized by 192 kJ mol^{-1} with respect to the separated reactants. The corresponding transition state lies 3 kJ mol^{-1} *lower* in energy than the separated reactants. In this sense, a barrier to addition does exist, but this barrier is located below the energy of the separated reactants and hence is called a *submerged barrier*. For the overall reaction from 9-phenanthrenyl plus vinylacetylene to intermediate **[2]**, the reaction is de facto barrier-less. The $C_{18}H_{13}$ intermediate **[2]** isomerizes via a hydrogen migration from the C10 carbon atom of the phenanthrenyl segment to the vinylacetylene moiety yielding **[3]**, thus effectively shifting the radical center from the aliphatic side chain to the aromatic ring. The latter undergoes a facile ring closure via a barrier of only 42 kJ mol^{-1} yielding intermediate **[4]** with the latter revealing the triphenylene carbon backbone. A second hydrogen migration – this time from the methylene moiety to the carbene carbon atom – is required to form intermediate **[5]**, which then undergoes hydrogen atom loss and aromatization to triphenylene ($C_{18}H_{12}$, **R1**) via a tight exit transition state located 23 kJ mol^{-1} above the separated products. The existence of a tight exit transition state, in which the hydrogen atom is emitted at an angle of 89° almost perpendicularly to the molecular plane, is sensible since the reversed reaction involves the addition of a hydrogen atom to a closed shell aromatic molecule, and a barrier of addition of a similar order of magnitude of 37 kJ mol^{-1} was computed for addition of atomic hydrogen to benzene – the prototype aromatic system.[13] Branched from intermediate **[2]** one isomer of triphenylene (*E*)-9-(but-1-en-3-yn-1-yl)-phenanthrene (**R2**) is produced from hydrogen loss of **[2]** via a barrier of 177 kJ mol^{-1}. Moreover, the van-der-Waals complex **[6]** can isomerize via addition of the radical center to the ethynyl moiety of the vinylacetylene molecule through a barrier of 13 kJ mol^{-1} leading to intermediate **[7]**, stabilized by 146 kJ mol^{-1} compared with the reactants, and further lose one hydrogen atom to yield the third isomer 9-(but-3-en-1-yn-1-yl)-phenanthrene (**R3**) via a tight exit transition state located 20 kJ mol^{-1} above the products. Consequently, the computational prediction of the formation of three structural isomers of $C_{18}H_{12}$ is well matched by our experimental studies and directly reflects two distinct entrance channels via two van-der-Waals complexes leading to three discrete structural isomers, defining a benchmark of a molecular mass growth process to PAHs.

An alternative possibility for the formation of triphenylene (**R1**) might be the reaction of phenanthryne with vinylacetyelene. Our calculations (Figure S4) reveal that **R1** can be plausibly produced in this reaction via vinylacetylene addition to the triple bond of phenanthryne, six-member ring closure and two hydrogen migrations after overcoming entrance barriers of 29-36 kJ mol^{-1}. However, according to the earlier calculations,[14] a rate constant for the hydrogen atom loss from an aryl radical to produce a triple bond in an aromatic ring (like in phenanthryne) is typically on the range of 10^3 s^{-1} under the conditions of the

present experiment making the lifetime of the aryl radical with respect to its decomposition to be ~1 ms, that is longer than the typical residence time in the reactor of a fes 10 µs. When phenanthryne is produced that late in the reactor, it may not have enough time to react with vinylacetylene and hence can be detected as in the present study. In the meantime, the phenanthryne plus vinylacetylene reaction cannot account for the formation of **R2** and **R3**, as no feasible pathways to these products could be found in our calculations of the pertinent potential energy surface (Figure S4).

hydrogen bond cleavage leading to 9-phenanthrenyl and phenyl, respectively, followed by formation of a weakly bound van-der-Waals complex, addition of the radical center to the methylene moiety of the vinylacetylene reactant via a submerged barrier, hydrogen shift from the aromatic moiety to the former vinylacetylene reactant establishing a second methylene group, ring closure, hydrogen shift, and eventually hydrogen atom loss followed by aromatization and formation of triphenylene and naphthalene, respectively. Consequently, the aforementioned features reveal that at ultralow temperatures in molecular clouds,

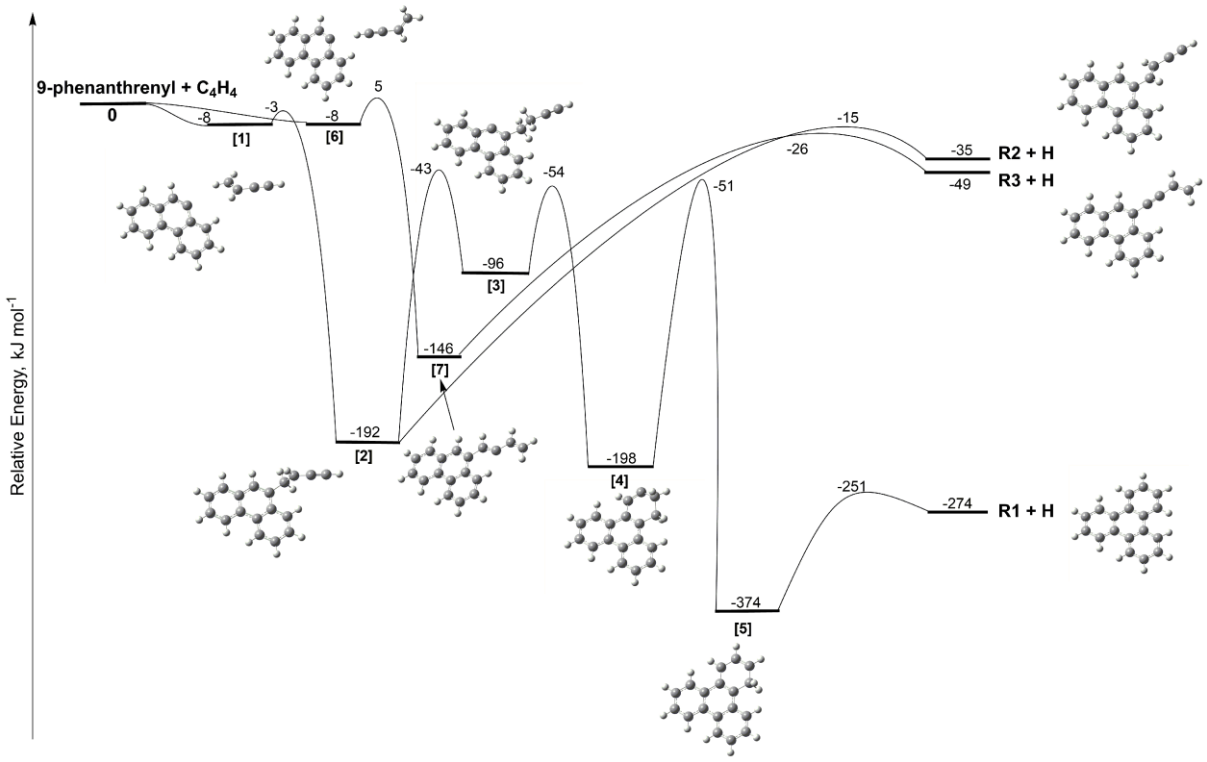

Figure 4. Potential energy surface (PES) for the 9-phenanthrenyl [$C_{14}H_9$]• reaction with vinylacetylene (C_4H_4) calculated at the G3(MP2,CC)//B3LYP/6-311G(d,p) level of theory leading to triphenylene (R1), (*E*)-9-(but-1-en-3-yn-1-yl)-phenanthrene (R2) and 9-(but-3-en-1-yn-1-yl)-phenanthrene (R3). The relative energies are given in kJ mol^{-1}.

This synthesis of triphenylene via ring expansion from 9-phenanthrenyl defines a standard de-facto *barrier-less* molecular mass growth process involving vinylacetylene addition followed by isomerization via hydrogen shifts and ring closure along with aromatization via atomic hydrogen loss. In cold molecular clouds such as Taurus Molecular Cloud -1 (TMC-1), the 9-phenanthrenyl-vinylacetylene route to triphenylene can be initiated by photolysis of phenanthrene ($C_{14}H_{10}$) by the internal ultraviolet field present even deep inside molecular clouds[15] thus leading, e.g., via atomic hydrogen loss from the C9-position to the 9-phenanthrenyl radical ([$C_{14}H_9$]•). Even at molecular cloud temperatures as low as 10 K, 9-phenanthrenyl reacts with vinylacetylene via a submerged barrier yielding eventually triphenylene via an overall exoergic bimolecular gas phase reaction. In these interstellar environments, the reaction mechanism of the phenanthrene – triphenylene ring expansion mirrors the benzene – naphthalene[6a] mass growth process starting with the photolysis of the aromatic precursor via carbon-HAVA might represent *the key mechanism* driving the molecular mass growth of PAHs via de facto barrier-less, successive ring expansions involving bimolecular reactions of aryl radical with vinylacetylene as a building block with the aryl radical generated from the corresponding aromatic precursor via photolysis by the internal ultraviolet field. However, at elevated temperatures such as in circumstellar envelopes of carbon stars of up to a few 1,000 K and in combustion flames, the reaction could be also initiated by hydrogen abstraction from phenanthrene followed by formation of triphenylene upon reaction with vinylacetylene. The critical role of the hydrogen abstraction – vinylacetylene addition (HAVA) mechanism in the 9-phenanthrenyl-vinylacetylene system to form triphenylene is based on the fact that the classical HACA route with the acetylene reactant *cannot* synthesize triphenylene, but rather produces acephenanthrylene ($C_{20}H_{12}$) in strong resemblance to the 1-naphthyl ([$C_{10}H_7$]•) – acetylene system leading to acenaphthylene thus blocking cyclization to a fourth six-membered ring (Figure 5).[6c] Likewise,

with just the HACA mechanism, the coronenyl radical ($[C_{24}H_{11}]^{\bullet}$) cannot generate higher PAHs containing solely six-membered rings, but leads to a PAH carrying a five-membered ring: cyclopenta[bc]coronene ($C_{26}H_{12}$) (Figure 6).

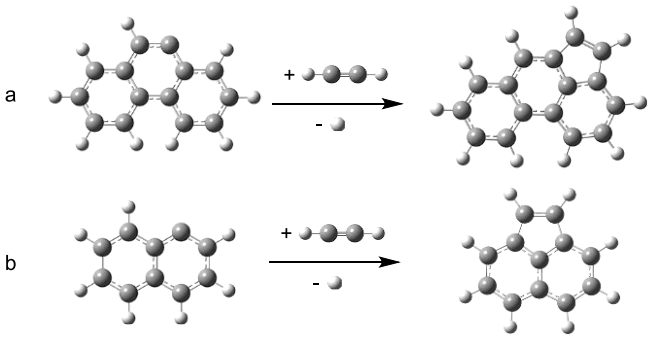

Figure 5. a) HACA mechanism involving the reaction of 9-phenanthrenyl ($[C_{14}H_9]^{\bullet}$) with acetylene (C_2H_2) to acephenanthrylene ($C_{16}H_{10}$) plus atomic hydrogen (H). b) HACA mechanism involving the reaction of 1-naphthyl ($[C_{10}H_7]^{\bullet}$) with acetylene (C_2H_2) to acenaphthylene ($C_{12}H_8$) plus atomic hydrogen (H).[5]

As reported in Parker et al.'s study on the formation of acenaphthylene ($C_{12}H_8$) from the reaction of 1-naphthyl ($[C_{10}H_7]^{\bullet}$) radical with acetylene (C_2H_2),[6c] which has an analogous bay structure as the 1-naphthyl radical, the 9-phenanthrenyl radical ($[C_{14}H_9]^{\bullet}$) is expected to react via a similar pathway with acetylene to produce acephenanthrylene ($C_{16}H_{10}$) along with atomic hydrogen, but not with two acetylene molecules to form triphenylene. It is noticeable that though no acephenanthrylene was observed under our experiment conditions, it is still a *potential* formation pathway as shown in Fig. 5a.

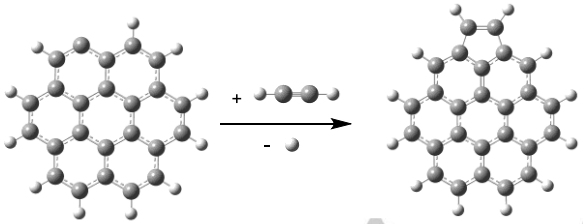

Figure 6. HACA reaction from coronenyl radical ($[C_{24}H_{11}]^{\bullet}$) to cyclopenta[bc]coronene ($C_{26}H_{12}$). Starting from the coronenyl radical, after addition of one acetylene molecule followed by atomic hydrogen, a five-member ring is generated,[6c] but no expansion occurs with an extra six-membered ring formation.

The pathways involve complementary HACA (red) and HAVA (blue) sequences with HACA leading to bay closure and HAVA supporting six-membered ring expansion eventually forming graphene-type nanostructures (Figure 7). The red and blue numbers within the benzene rings define the step in the growth sequence. Considering the molecular structures D_{3h} symmetric triphenylene and D_{6h} symmetric coronene molecule, a hydrogen abstraction from any of the six bay carbon atoms in triphenylene followed by acetylene addition could lead to bay closure via HACA similarly as verified in the reaction of the biphenylyl radical (C_6H_5-C_6H_4) and 4-phenanthrenyl radical with acetylene leading to phenanthrene ($C_{14}H_{10}$)[6d] and pyrene ($C_{16}H_{10}$),[10] respectively. Overall, three repetitive HACA sequences could form ultimately coronene from triphenylene. The subsequent molecular growth processes of coronene are rather tricky. HACA – initiated via abstraction of any of the chemically equivalent hydrogen atoms of coronene – does not lead to the growth of a six-membered ring (Figure S4); the abstraction of a hydrogen atom leads essentially to a 1-naphthyl moiety, which has been shown to react with acetylene to form a five-membered ring such as in acenaphthylene synthesized in the 1-naphthyl ($C_{10}H_7$) – acetylene system.[6c] On the other hand, a transfer of the aforementioned HAVA pathway to coronene suggests that three repetitive HAVA sequences can form three six-membered rings yielding eventually tribenzo[fgh,pqr,za1b1]trinaphthylene ($C_{36}H_{18}$). From here, additional HACA pathways can take over forming circumcoronene via diphenanthro[3,4,5,6-efghi:3',4',5',6'-uvabc]ovalene ($C_{48}H_{18}$). This reaction sequence also backs up Naraoka et al.'s results of a detailed $^{13}C/^{12}C$ isotopic analysis of PAHs in meteorites such as in Asuka-881458 identifying triphenylene as a key PAH on the path to more complex structures consisting of fused benzene rings possibly leading to the build-up of two-dimensional graphene-type nanostructures.[1] Here, starting essentially from triphenylene, HAVA pathways result in acene-type growth patterns in three sectors of the molecular plane separated by 120°, whereas the classical HACA mechanisms close the bays.

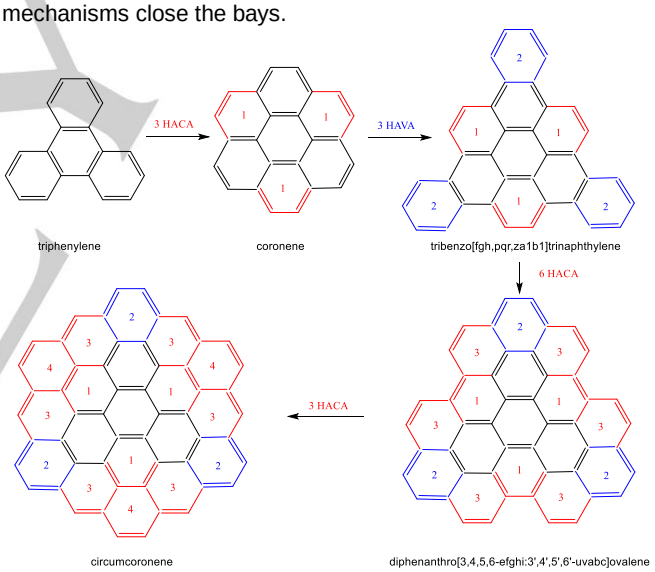

Figure 7. Potential schematic mass growth processes starting with triphenylene ($C_{18}H_{12}$) to circumcoronene ($C_{54}H_{18}$) via tandem HACA and HAVA reactions. These mass growth processes have not been studied experimentally yet.

To conclude, the facile route to triphenylene ($C_{18}H_{12}$), as identified in carbonaceous chondrites, via the bimolecular reaction of the 9-phenanthrenyl radical with vinylacetylene following the hydrogen abstraction – vinylacetylene addition (HAVA) mechanism represents the prototype of a *barrier-less* reaction leading through submerged barriers and resonantly stabilized free radical (RSFR) intermediates to facile molecular growth processes in PAHs via ring expansion through a bimolecular collision at temperatures as low as 10 K. Therefore, HAVA represents *the key mechanism* driving the molecular mass growth processes of PAHs via de facto barrier-less, successive ring expansions involving bimolecular reactions of

aryl radical with vinylacetylene as a molecular building block. Starting from triphenylene - HAVA and HACA may even operate in tandem to eventually synthesize graphene-type nanostructures and after condensation of multiple layers graphitized carbon as identified in carbonaceous chondrites like Allende[16] ultimately changing our paradigm on the interstellar carbon chemistry and the progression of carbonaceous matter in the universe on the most fundamental, microscopic level.

Method - Experimental

The experiments were conducted at the Advanced Light Source (ALS) at the Chemical Dynamics Beamline (9.0.2.) exploiting a high-temperature chemical reactor consisting of a resistively-heated silicon carbide (SiC) tube of 20 mm length and 1 mm inner diameter.[6c, 6d, 17] This reactor is incorporated into a molecular beam apparatus operated with a Wiley-McLaren reflectron time-of-flight mass spectrometer (Re-TOF-MS). This setup investigates discrete chemical reactions to simulate PAH growth *in situ* through the reaction of radicals. Here, 9-phenanthrenyl radicals [$C_{14}H_9$]$^{\bullet}$ were prepared at the concentration of less than 0.1% *in situ* via pyrolysis of the 9-bromophenanthrene precursor ($C_{14}H_9Br$; TCI-America, > 98%) seeded in vinylacetylene/helium (5% C_4H_4; 95% He; Airgas) carrier gas at a pressure of 300 Torr. The temperature of the SiC tube was monitored using a Type-C thermocouple and was maintained at 1450 ± 10 K. At this temperature, 9-bromophenanthrene dissociates to the 9-phenanthrenyl radical plus atomic bromine *in situ* and reacts with vinylacetylene, and the target signal of *m/z* = 228 was the strongest compared with those at other temperatures. The reaction products synthesized in the reactor were expanded supersonically and passed through a 2-mm diameter skimmer located 10 mm downstream the pyrolytic reactor and enter the main chamber, which houses the Re-TOF-MS. The products within the supersonic beam were then photoionized in the extraction region of the spectrometer by exploiting quasi-continuous tunable synchrotron vacuum ultraviolet (VUV) light and detected with a microchannel plate (MCP). It is important to highlight that VUV single photon ionization represents essentially a fragment-free ionization technique and hence is characterized as a *soft ionization* method[18] compared to electron impact ionization, with the latter leading to excessive fragmentation of the parent ion. The ions formed via photoionization are extracted and fed onto a microchannel plate detector through an ion lens. Photoionization efficiency (PIE) curves, which report ion counts as a function of photon energy from 7.30 eV to 10.00 eV with a step interval of 0.05 eV at a well-defined mass-to-charge ratio (*m/z*), were produced by integrating the signal recorded at the specific *m/z* for the species of interest and normalized to the incident photon flux. The residence time in the reactor tube under our experimental condition are tens to hundreds of µs.[19] Reference (blank) experiments were also conducted by expanding neat helium carrier gas with the 9-bromophenanthrene precursor into the resistively-heated SiC tube. No signals which can be associated with the $C_{18}H_{12}$ isomers at *m/z* = 202 or 203 was observed in these control experiments. For the PIE calibration compounds, triphenylene (R1) was purchased from TCI America (96%); (*E*)-9-(But-1-en-3-yn-1-yl)-phenanthrene (R2) and 9-(but-3-en-1-yn-1-yl)-phenanthrene (R3) were newly synthesized in this work.

Method - Electronic Structure Calculations

The energies and molecular parameters of the local minima and transition states involved in the reaction were computed at the G3(MP2,CC)//B3LYP/6-311G(d,p) level of theory[20] within a chemical accuracy of 3–6 kJ mol^{-1} for the relative energies and 0.01–0.02 Å for bond lengths as well as 1–2° for bond angles.[20c] Vertical and adiabatic ionization energies were also computed at the G3(MP2,CC)//B3LYP/6-311G(d,p) level of theory. The GAUSSIAN 09[21] and MOLPRO 2010 program packages[22] were utilized for the ab initio calculations.

Acknowledgements

This work was supported by the US Department of Energy, Basic Energy Sciences DE-FG02-03ER15411 (experimental studies) and DE-FG02-04ER15570 (computational studies and organic synthesis of 9-(but-3-en-1-yn-1-yl)-phenanthrene and (*E*)-9-(but-1-en-3-yn-1-yl)-phenanthrene) to the University of Hawaii and Florida International University, respectively. Ab initio calculations of the $C_{18}H_{13}$ PES relevant to the reaction of 9-phenanthrenyl radical with vinylacetylene at Samara University were supported by the Ministry of Education and Science of the Russian Federation under Grant No. 14.Y26.31.0020. MA, UA, BX, and the experiments at the chemical dynamics beamline at the ALS are supported by the Director, Office of Science, Office of Basic Energy Sciences, of the U.S. Department of Energy under Contract No. DE-AC02-05CH11231, through the Gas Phase Chemical Physics Program, Chemical Sciences Division.

Keywords: Hydrogen Abstraction – Vinylacetylene Addition (HAVA) • polycyclic aromatic hydrocarbons • gas-phase chemistry • mass spectrometry • interstellar medium

[1] H. Naraoka, A. Shimoyama, K. Harada, *Earth Planet. Sci. Lett.* **2000**, *184*, 1-7.
[2] a) L. Becker, T. E. Bunch, *Meteorit. Planet. Sci.* **1997**, *32*, 479-487; b) M. P. Callahan, A. Abo-Riziq, B. Crews, L. Grace, M. S. de Vries, *Spectrochim. Acta A* **2008**, *71*, 1492-1495.
[3] R. Gredel, Y. Carpentier, G. Rouillé, M. Steglich, F. Huisken, T. Henning, *Astron. Astrophys.* **2011**, *530*, A26.
[4] a) I. Gilmour, C. T. Pillinger, *Mon. Notices Royal Astron. Soc.* **1994**, *269*, 235-240; b) H. Naraoka, A. Shimoyama, K. Harada, *Mineral. Mag.* **1998**, *62A*, 1056-1057; c) A. G. G. M. Tielens, *Annu. Rev. Astron. Astrophys.* **2008**, *46*, 289-337; d) A. G. G. M. Tielens, L. J. Allamandola, Pan Stanford Publishing Pte. Ltd., **2011**, pp. 341-380; e) A. G. G. M. Tielens, *Rev. Mod. Phys.* **2013**, *85*, 1021-1081.
[5] a) I. Ristorcelli, A. Klotz, *Astron. Astrophys.* **1997**, *317*, 962-967; b) M. Y. Zolotov, E. L. Shock, *Meteorit. Planet. Sci.* **2000**, *35*, 629-638.
[6] a) D. S. Parker, F. Zhang, Y. S. Kim, R. I. Kaiser, A. Landera, V. V. Kislov, A. M. Mebel, A. Tielens, *Proc. Nat. Acad. Sci. U.S.A.* **2012**, *109*, 53-58; b) D. S. Parker, R. I. Kaiser, T. P. Troy, M. Ahmed, *Angew. Chem. Int. Edit.* **2014**, *53*, 7740-7744; c) D. S. N. Parker, R. I. Kaiser, B. Bandyopadhyay, O. Kostko, T. P. Troy, M. Ahmed, *Angew. Chem. Int. Edit.* **2015**, *54*, 5421-5424; d) T. Yang, R. I. Kaiser, T. P. Troy, B. Xu, O. Kostko, M. Ahmed, A. M. Mebel, M. V. Zagidullin, V. N. Azyazov, *Angew. Chem. Int. Edit.* **2017**, *56*, 4515-4519.
[7] M. Frenklach, H. Wang, *Proc. Combust. Inst.* **1991**, *23*, 1559-1566.
[8] a) M. Frenklach, E. D. Feigelson, *Astrophys. J.* **1989**, *341*, 372-384; b) H. Richter, J. B. Howard, *Prog. Energy Combust. Sci.* **2000**, *26*, 565-608; c) M. Frenklach, *Phys. Chem. Chem. Phys.* **2002**, *4*, 2028-2037.
[9] a) J. D. Bittner, J. B. Howard, *Proc. Combust. Inst.* **1981**, *18*, 1105-1116; b) J. Appel, H. Bockhorn, M. Frenklach, *Combust. Flame* **2000**, *121*, 122-136.
[10] L. Zhao, R. I. Kaiser, B. Xu, U. Ablikim, M. Ahmed, D. Joshi, G. Veber, F. R. Fischer, A. M. Mebel, *Nat. Astron.* **2018**, *2*, 413-419.
[11] a) C.-H. Chin, W.-K. Chen, W.-J. Huang, Y.-C. Lin, S.-H. Lee, *Icarus* **2013**, *222*, 254-262; b) A. Coustenis, A. Salama, B. Schulz, S. Ott, E. Lellouch, T. h. Encrenaz, D. Gautier, H. Feuchtgruber, *Icarus* **2003**, *161*, 383-403.
[12] a) R. I. Kaiser, D. S. N. Parker, A. M. Mebel, *Annu. Rev. Phys. Chem.* **2015**, *66*, 43-67; b) A. M. Mebel, A. Landera, R. I. Kaiser, *J. Phys. Chem. A* **2017**, *121*, 901-926.
[13] A. M. Mebel, M. C. Lin, T. Yu, K. Morokuma, *J. Phys. Chem. A* **1997**, *101*, 3189-3196.
[14] A. M. Mebel, Y. Georgievskii, A. W. Jasper, S. J. Klippenstein, *Proc. Combust. Inst.* **2017**, *36*, 919-926.

[15] a) S. Schlemmer, D. Cook, J. Harrison, B. Wurfel, W. Chapman, R. Saykally, *Science* **1994**, *265*, 1686-1689; b) M. P. Bernstein, S. A. Sandford, L. J. Allamandola, J. S. Gillette, S. J. Clemett, R. N. Zare, *Science* **1999**, *283*, 1135-1138; c) W. Schutte, M. Greenberg, *NASA Conf. Publ.* **1989**, *3036*, 267-268.

[16] a) S. Messenger, S. Amari, X. Gao, R. M. Walker, S. J. Clemett, X. D. F. Chillier, R. N. Zare, R. S. Lewis, *Astrophys. J.* **1998**, *502*, 284-295; b) S. Mostefaoui, P. Hoppe, A. El Goresy, *Science* **1998**, *280*, 1418-1420; c) P. P. K. Smith, P. R. Buseck, *Geochim. Cosmochim. Acta, Suppl.* **1982**, *16*, 1167-1175; d) U. Ott, *Space Sci. Rev.* **2007**, *130*, 87-95; e) W. W. Duley, *Astrophys. J.* **2000**, *528*, 841-848; f) S. Amari, R. S. Lewis, E. Anders, *Geochim. Cosmochim. Acta* **1995**, *59*, 1411-1426; g) E. Zinner, S. Amari, B. Wopenka, R. S. Lewis, *Meteoritics* **1995**, *30*, 209-226.

[17] F. T. Zhang, R. I. Kaiser, V. V. Kislov, A. M. Mebel, A. Golan, M. Ahmed, *J. Phys. Chem. Lett.* **2011**, *2*, 1731-1735.

[18] a) F. Qi, *Proc. Combust. Inst.* **2013**, *34*, 33-63; b) T. A. Cool, A. McIlroy, F. Qi, P. R. Westmoreland, L. Poisson, D. S. Peterka, M. Ahmed, *Rev. Sci. Instrum.* **2005**, *76*, 094102.

[19] Q. Guan, K. N. Urness, T. K. Ormond, D. E. David, G. Barney Ellison, J. W. Daily, *Int. Rev. Phys. Chem.* **2014**, *33*, 447-487.

[20] a) L. A. Curtiss, K. Raghavachari, P. C. Redfern, V. Rassolov, J. A. Pople, *J. Chem. Phys.* **1998**, *109*, 7764-7776; b) A. G. Baboul, L. A. Curtiss, P. C. Redfern, K. Raghavachari, *J. Chem. Phys.* **1999**, *110*, 7650-7657; c) L. A. Curtiss, K. Raghavachari, P. C. Redfern, A. G. Baboul, J. A. Pople, *Chem. Phys. Lett.* **1999**, *314*, 101-107.

[21] M. J. Frisch, G. W. Trucks, H. B. Schlegel, G. E. Scuseria, M. A. Robb, J. R. Cheeseman, G. Scalmani, V. Barone, B. Mennucci, G. A. Petersson, H. Nakatsuji, M. Caricato, X. Li, H. P. Hratchian, A. F. Izmaylov, J. Bloino, G. Zheng, J. L. Sonnenberg, M. Hada, M. Ehara, K. Toyota, R. Fukuda, J. Hasegawa, M. Ishida, T. Nakajima, Y. Honda, O. Kitao, H. Nakai, T. Vreven, J. A. Montgomery, Jr., J. E. Peralta, F. Ogliaro, M. Bearpark, J. J. Heyd, E. Brothers, K. N. Kudin, V. N. Staroverov, T. Keith, R. Kobayashi, J. Normand, K. Raghavachari, A. Rendell, J. C. Burant, S. S. Iyengar, J. Tomasi, M. Cossi, N. Rega, J. M. Millam, M. Klene, J. E. Knox, J. B. Cross, V. Bakken, C. Adamo, J. Jaramillo, R. Gomperts, R. E. Stratmann, O. Yazyev, A. J. Austin, R. Cammi, C. Pomelli, J. W. Ochterski, R. L. Martin, K. Morokuma, V. G. Zakrzewski, G. A. Voth, P. Salvador, J. J. Dannenberg, S. Dapprich, A. D. Daniels, O. Farkas, J. B. Foresman, J. V. Ortiz, J. Cioslowski, D. J. Fox, *Gaussian 09, Revision A.1 Gaussian Inc., Wallingford CT* **2009**.

[22] H. J. Werner, P. J. Knowles, G. Knizia, F. R. Manby, M. Schütz, P. Celani, W. Györffy, D. Kats, T. Korona, R. Lindh, A. Mitrushenkov, G. Rauhut, K. R. Shamasundar, T. B. Adler, R. D. Amos, A. Bernhardsson, A. Berning, D. L. Cooper, M. J. O. Deegan, A. J. Dobbyn, F. Eckert, E. Goll, C. Hampel, A. Hesselmann, G. Hetzer, T. Hrenar, G. Jansen, C. Köppl, Y. Liu, A. W. Lloyd, R. A. Mata, A. J. May, S. J. McNicholas, W. Meyer, M. E. Mura, A. Nicklaß, D. P. O'Neill, P. Palmieri, D. Peng, K. Pflüger, R. Pitzer, M. Reiher, T. Shiozaki, H. Stoll, A. J. Stone, R. Tarroni, T. Thorsteinsson, M. Wang, *MOLPRO, version 2010.1, a package of ab initio programs,* http://www.molpro.net.

Entry for the Table of Contents

COMMUNICATION

The triphenylene molecule – a potential precursor to two dimensional graphite nano sheets in the interstellar medium – can be formed without entrance barrier at temperatures as low as 10 K in molecular clouds.

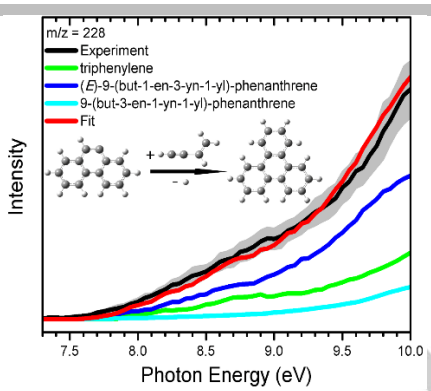

Long Zhao, Bo Xu, Utuq Ablikim, Wenchao Lu, Musahid Ahmed, Mikhail M. Evseev, Eugene K. Bashkirov, Valeriy N. Azyazov, A. Hasan Howlader, Stanislaw F. Wnuk, Alexander M. Mebel,* Ralf I. Kaiser**

Page No. – Page No.

Gas Phase Synthesis of Triphenylene ($C_{18}H_{12}$)

Supporting Information

Gas Phase Synthesis of Triphenylene ($C_{18}H_{12}$)

Long Zhao,[a] Bo Xu,[b] Utuq Ablikim,[b] Wenchao Lu,[b] Musahid Ahmed,[b,*] Mikhail M. Evseev,[c] Eugene K. Bashkirov,[c] Valeriy N. Azyazov,[c,d] A. Hasan Howlader,[e] Stanislaw F. Wnuk,[e] Alexander M. Mebel,[c,e,*] Ralf I. Kaiser[a*]

[a] Department of Chemistry, University of Hawaii at Manoa, Honolulu, Hawaii, 96822 (USA)

[b] Chemical Sciences Division, Lawrence Berkeley National Laboratory, Berkeley, CA 94720 (USA)

[c] Samara National Research University, Samara 443086 (Russia)

[d] Department of Chemical & Electric Discharge Lasers, Lebedev Physical Institute of RAS, Samara 443011 (Russia)

[e] Department of Chemistry and Biochemistry, Florida International University, Miami, FL 33199 (USA)

[*] Corresponding authors:
Ralf I. Kaiser <ralfk@hawaii.edu>
Musahid Ahmed <mahmed@lbl.gov>
Alexander M. Mebel <mebela@fiu.edu>

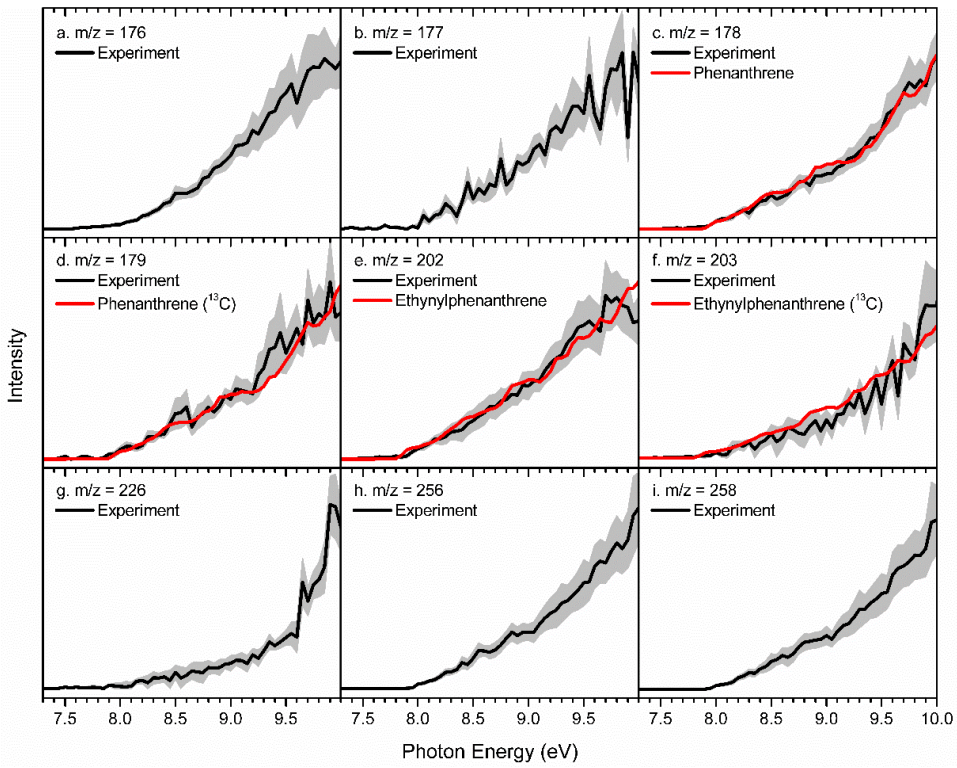

Figure S1. PIE curves of distinct ions detected in 9-phenanthrenyl - vinylacetylene system.

Signal at *m/z* = 202 and 203 can be associated with $C_{16}H_{10}$ molecule(s) and the ^{13}C-isotopially substituted counterpart(s) $^{13}CC_{15}H_{10}$, respectively. After scaling, both data sets are superimposable verifying that signals at *m/z* = 202 and 203 originate from the same (isotopically substituted) isomer. This signal can be fit with the PIE curve of ethynylphenanthrene. Since the adiabatic ionization energies of distinct ethynylphenanthrene isomers are around 7.8 eV, and their PIE curves are similar, the present work does not allow an identification of the specific ethynylphenanthrene isomer(s) formed. Here, at elevated temperatures, vinylacetylene can be pyrolyzed at a level of about 2% forming two acetylene molecules, which can react with 9-phenanthrene via acetylene addition followed by hydrogen loss yielding ethynylphenanthrene.[1] Alternatively, acetylene can be formed as a product of the H + C_4H_4 reaction. Note that acephenanthrylene (an isomer of ethynylphenanthrene which can potentially be formed by a five-member ring closure and aromatization via hydrogen atom loss following acetylene addition) was not observed under present experimental conditions. Signal at *m/z* = 177 can be connected to the 9-phenanthrenyl radical. *m/z* = 176 and *m/z* = 178 origin from the hydrogen atom loss and hydrogen atom addition of 9-phenanthrenyl leading to phenanthryne isomers and phenanthrene, respectively. *m/z* = 178

and 179 can be both fit with the reference PIE curve of phenanthrene, verifying they are both attributed to phenanthrene with m/z = 179 resembling the ^{13}C-substituted phenanthrene.

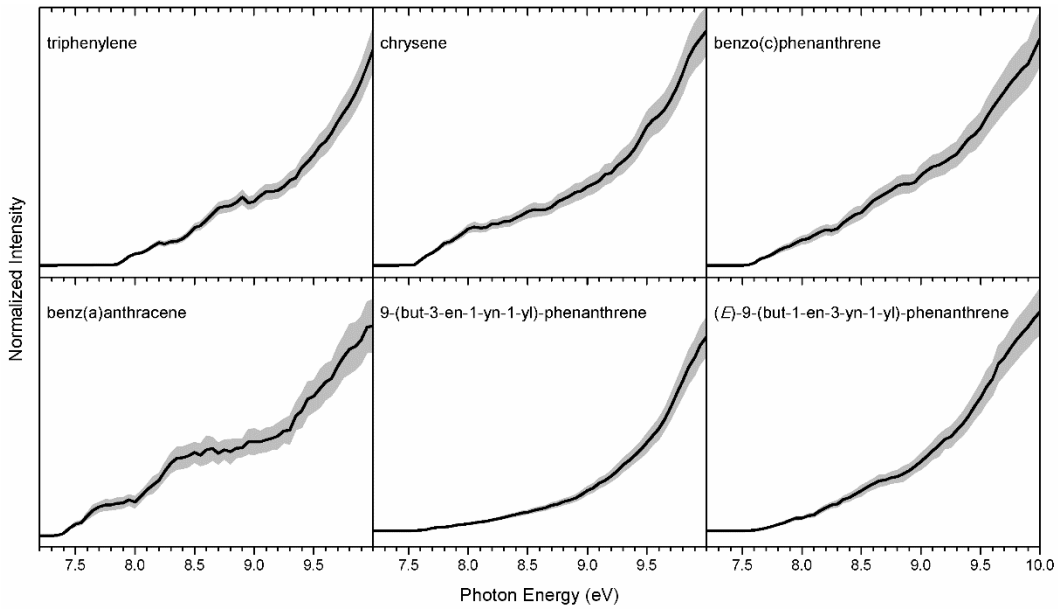

Figure S2. PIE calibration curves for distinct $C_{18}H_{12}$ isomers: triphenylene, chrysene, benzo(c)phenanthrene, benz(a)anthracene, 9-(but-3-en-1-yn-1-yl)-phenanthrene and (*E*)-9-(but-1-en-3-yn-1-yl)-phenanthrene.

These PIE calibration curves were newly recorded in this work and are shown as black along with the error limits (grey area). The adiabatic ionization energies of these isomers are 7.70 ± 0.05, 7.55 ± 0.05, 7.55 ±0.05, 7.35 ± 0.05 eV, 7.60 ± 0.05 eV and 7.60 ± 0.05 eV, respectively, comparing with literature values of 7.84 ± 0.01[2], 7.60 ± 0.01[3], 7.60 ± 0.02[4] and 7.41 ± 0.02[4] for the first four isomers. The overall error bars consist of two parts: ±10% based on the accuracy of the photodiode and a 1 σ error of the PIE curve averaged over the individual scans.

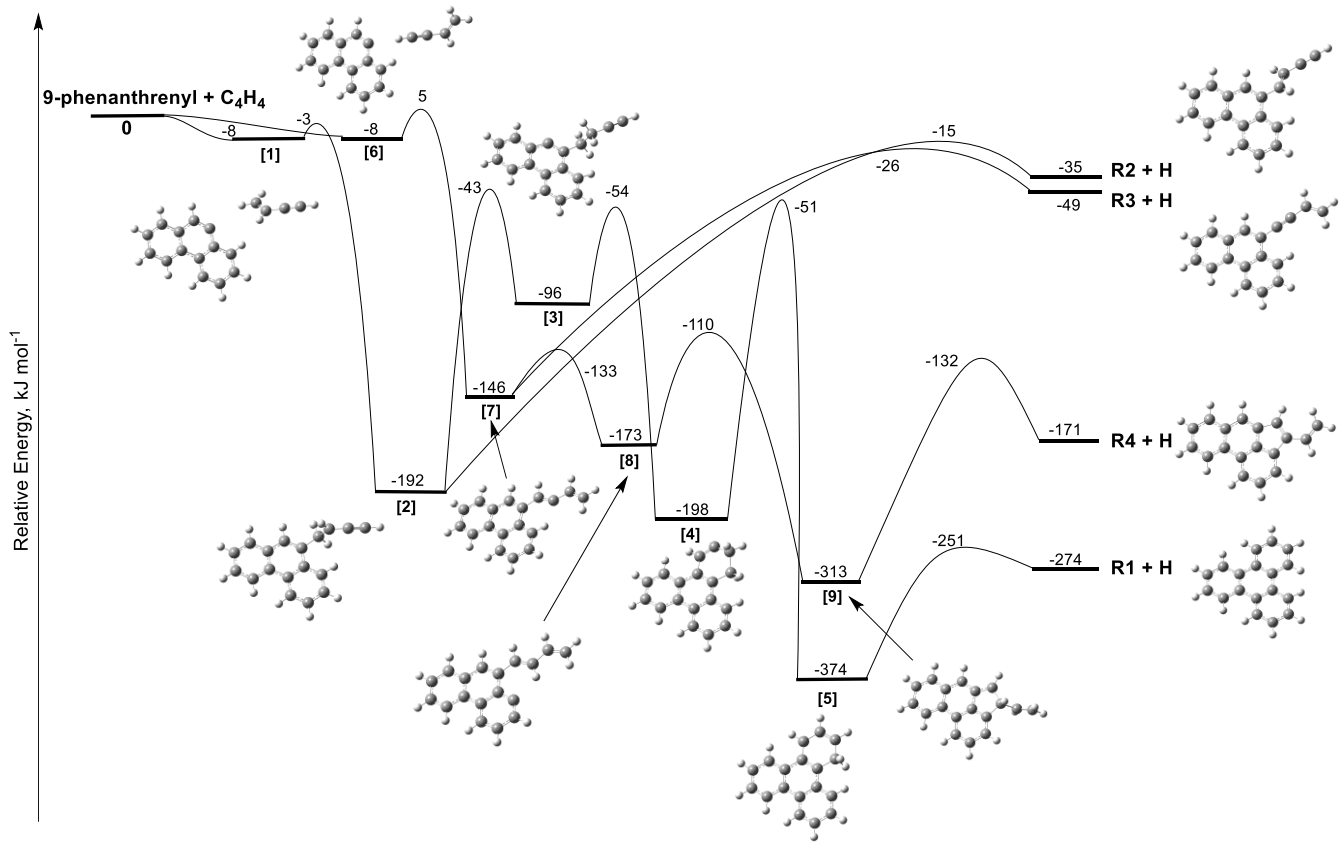

Figure S3. Potential energy surface (PES) for the 9-phenanthrenyl $[C_{14}H_9]^{\bullet}$ reaction with vinylacetylene (C_4H_4) including an additional energetically favorable pathway forming a product R4 (4-vinylacephenanthrylene) calculated at the G3(MP2,CC)//B3LYP/6-311G(d,p) level of theory. The relative energies are given in kJ mol^{-1}. Since the calculated adiabatic ionization energy of R4 is 7.35±0.10 eV, a small contribution of this product to the experimental PIE at energies below 7.6 eV (see Fig. 3) cannot be completely ruled out.

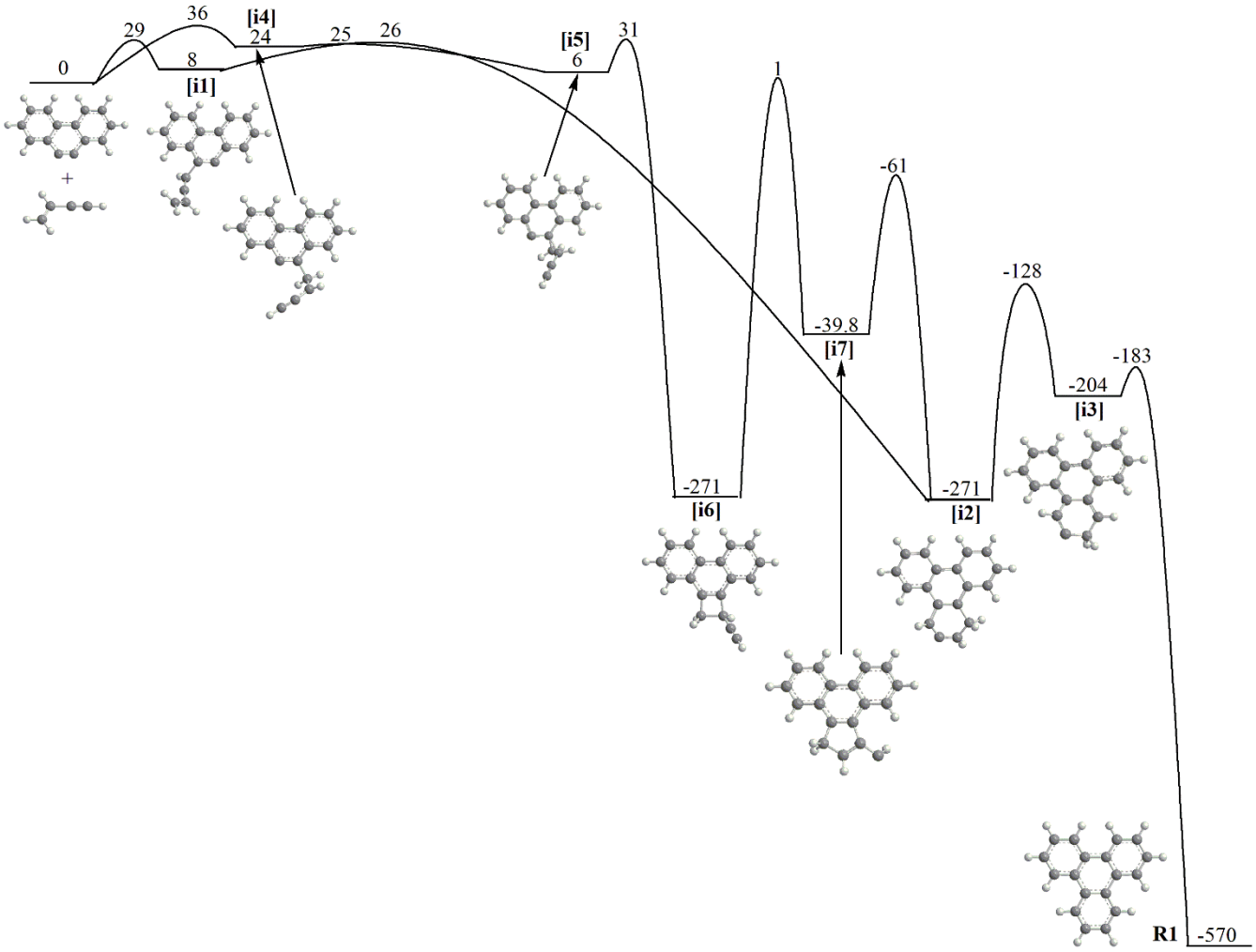

Figure S4. PES for the phenanthryne ($C_{14}H_8$) reaction with vinylacetylene (C_4H_4) calculated at the B3LYP/6-311G(d,p) level of theory. The relative energies are given in kJ mol^{-1}.

The reaction begins with the addition of vinylacetylene to the triple bond of phenanthryne. When the addition occurs by the acetylenic end of C_4H_4, the formation of the initial complex **[i1]** is immediately followed by six-member ring closure to **[i2]** and then, two H migrations in the new ring via **[i3]** lead to its aromatization and the formation of triphenylene (**R1**). The highest barrier on the phenanthryne + C_4H_4 → **[i1]** → **[i2]** → **[i3]** → **R1** pathway, 29 kJ mol^{-1}, is found for the entrance step. Alternatively, when the addition occurs by the vinylic end of C_4H_4 to form **[i4]** via a 36 kJ mol^{-1} barrier, the ring closure mechanism is more complex; a three-member ring is formed first in **[i5]** and then it stepwisely expands to four- (**[i6]**), five- (**[i7]**), and finally six-member ring in **[i2**]. No pathways involving H migrations without the extra ring closure and leading to **R2** or **R3** could be found and thus, the phenanthryne plus vinylacetylene reaction cannot account for these products observed in experiment.

The mechanism explored here deserves further detailed consideration at a higher level of theory and rate constant calculations, especially for the prototype benzyne (C_6H_4) + vinylacetylene reaction, because our results demonstrate that the reactions of aromatic alkynes with C_4H_4 may represent a plausible mechanism for PAH growth under high-temperature (combustion) conditions. However, due to the significant entrance barriers, this mechanism is not feasible in the interstellar medium.

Synthesis of (*E*)-9-(But-1-en-3-yn-1-yl)-phenanthrene (R2)

(*E*)-9-(But-1-en-3-yn-1-yl)-phenanthrene **(R2)** was synthesized by stereoselective conversion of 9-ethynylphenanthrene into *trans*-1-alkenyliodide via hydroboration-hydrolysis-iodination[5] sequence followed by Sonogashira cross-coupling reaction with (trimethylsilyl)acetylene (**Scheme 1**).

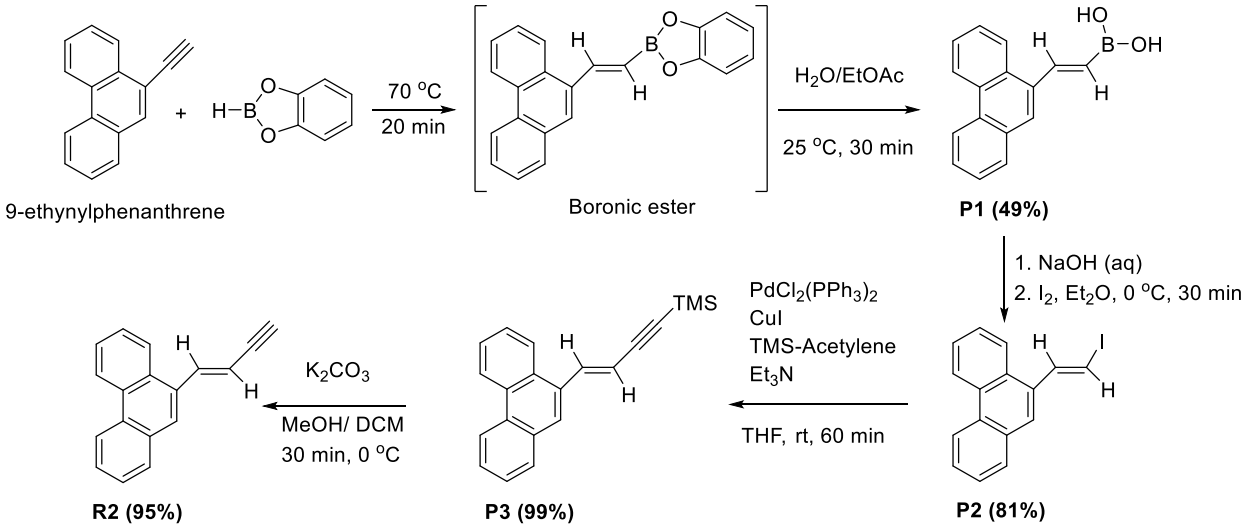

Scheme 1. Synthesis of (*E*)-9-(but-1-en-3-yn-1-yl)-phenanthrene (**R2**).

1. (*E*)-(2-(Phenanthren-9-yl)-vinyl)-boronic acid (P1)

9-Ethynylphenanthrene (505.5 mg, 2.5 mmol) and catecholborane (266 µL, 300 mg, 2.5 mmol) were placed in a flame-dried flask under N_2 at ambient temperature and the reaction mixture were stirred for 20 min at 70 °C. Within this 20 min, the reaction mixture forms a small lump and was kept few minutes at ambient temperature. Then H_2O/EtOAc (1:1; 10 mL) were added into the reaction mixture and stirred for 30 min at 25 °C to effect the hydrolysis of boronic ester. The reaction mixture was extracted with EtOAc, organic layer separated and the aqueous layer was extracted with EtOAc two more times. The combined organic layer was dried (Na_2SO_4) and evaporated. The residue was column chromatographed (20-40% EtOAc in hexane) to give **P1** (301 mg, 49%) as white powder: ^{1}H NMR (DMSO-d_6, 400 MHz) δ 6.32 (d, J = 18.0 Hz, 1H), 7.63-7.76 (m, 4H), 7.98 (s, 2H), 8.04 (d, J = 8.8 Hz, 2H), 8.13 (d, J = 18.0 Hz, 1H), 8.32-8.34 (m, 1H), 8.79-8.82 (m, 1H), 8.88-8.90 (m, 1H); ^{13}C NMR (DMSO-d_6, 100.6 MHz): δ 122.66, 122.86, 123.36, 123.55, 124.12, 124.15, 126.98, 127.05, 128.90, 129.81, 129.85, 129.88, 131.23, 134.26, 143.09, 145.27.

2. (*E*)-9-(2-iodovinyl)-phenanthrene (P2)

The boronic acid **P1** (100 mg, 0.40 mmol) was dissolved in 5 mL Et_2O in a 50 mL flask and cooled to 0 ^oC. Then aqueous NaOH (400 µL, 3 N, 1.2 mmol) was added dropwise followed by elemental iodine (121.8 mg, 0.48 mmol) dissolved in 5 mL Et_2O, while stirring at 0 ^oC. The reaction mixture was stirred for 30 min at 0 ^oC and the excess I_2 was destroyed by aqueous $Na_2S_2O_3$ solution. The reaction mixture was extracted with Et_2O and organic layer was separated and the aqueous layer was extracted with Et_2O twice. The combined organic layer was dried (Na_2SO_4) and evaporated. The residue was column chromatographed (*n*-hexane) to give **P2** (108 mg, 81%) as white powder: ^1H NMR ($CDCl_3$, 400 MHz) δ 6.93 (d, J = 14.8 Hz, 1H), 7.58-7.71 (m, 4H), 7.75 (s, 1H), 7.89 (d, J = 7.6 Hz, 1H), 8.09 (d, J = 8.0 Hz, 1H), 8.16 (d, J = 14.4 Hz, 1H), 8.65 (d, J = 8.4 Hz, 1H), 8.72 (d, J = 7.6 Hz, 1H); ^{13}C NMR ($CDCl_3$, 100.6 MHz): δ 122.63, 122.85, 123.13, 123.37, 124.72, 125.53, 125.66, 127.06, 128.94, 129.67, 130.49, 130.55, 131.65, 134.85, 143.58, 143.61.

3. (*E*)-Trimethyl-(4-(phenanthren-9-yl)-but-3-en-1-yn-yl)-silane (P3)

$Pd(PPh_3)_2Cl_2$ (8.4 mg, 0.012 mmol) and Cu(I)I (4.6 mg, 0.024 mmol) were added to dry THF (5 mL) in a flame-dried round bottom flask equipped with a stir bar under N_2 at 0 ^oC (ice-bath). Then **P2** (100 mg, 0.30 mmol) was added followed by TMS-acetylene (62 µL, 44 mg, 0.45 mmol) and Et_3N (84 µL, 61 mg, 0.60 mmol). The resulting mixture was allowed to warm up to ambient temperature and was stirred for 1h. [progress of the reaction was monitored by TLC (*n*-hexane)]. Volatiles were evaporated and the residue was column chromatographed (*n*-hexane) to give **P3** as light yellow gummy solid (90 mg, 99%).^1H NMR: ($CDCl_3$, 400 MHz) δ 0.30 (s, 9H), 6.34 (d, J = 16.0 Hz, 1H), 7.58-7.67 (m, 4H), 7.81 (d, J = 16.0 Hz, 1H), 7.85 (s, 1H), 7.88 (d, J = 7.6 Hz, 1H), 8.17 (d, J = 9.2 Hz, 1H), 8.65 (d, J = 8.0 Hz, 1H), 8.72 (d, J = 9.2 Hz, 1H).

4. (*E*)-9-(But-1-en-3-yn-1-yl)-phenanthrene (R2)

Anhydrous K_2CO_3 (41 mg, 0.3 mmol) was added to a stirred solution of **P3** (80 mg, 0.27 mmol) in 4 mL MeOH/DCM (1:1) at room temperature. After 30 min, volatiles were evaporated and the residue was column chromatographed (*n*-hexane) to give **R2** (58 mg, 95%) as light yellow powder. ^1H NMR: ($CDCl_3$, 400 MHz) δ 3.12 (d, J = 2.4 Hz, 1H), 6.29 (dd, J = 16.0, 2.4 Hz, 1H), 7.58-7.67 (m, 4H), 7.83-7.90 (m, 3H), 8.13-8.16 (m, 1H), 8.66 (d, J = 8.0 Hz, 1H), 8.72-8.74 (m, 1H); ^{13}C NMR ($CDCl_3$, 100.6 MHz): δ

79.17, 83.13, 110.41, 122.61, 122.85, 123.21, 123.38, 124.55, 125.10, 126.99, 129.07, 130.10, 130.53, 131.80, 131.57, 132.57, 141.05, 141.13.

In summary, treatment of 9-ethynylphenanthrene with catecholborane at 70 ^{o}C form intermediary boronic ester, which was hydrolyzed with H_2O to give *trans*-alkenylboronic acid, **P1** in 49% yield after purification on silica gel column. Treatment of the purified (catechol free) **P1** in ether solution with iodine (1.2 equiv) in the presence of aqueous NaOH (3.0 equiv) at 0 ^{o}C provided alkenyliodide **P2** (81%). Subsequent Sonogashira coupling of **P2** with (trimethylsilyl)acetylene yielded **P3** (99%), which on desilylation with K_2CO_3 in MeOH/DCM gave desired **R2** (95% yield). It is noteworthy that our attempts to synthesize alkenyl bromide analogue of **P2** directly from 9-ethynylphenanthrene by adopting reported hydrobromination conditions[6] failed giving instead the alkene analogue.

Synthesis of 9-(But-3-en-1-yn-1-yl)-phenanthrene (R3)

9-(but-3-en-1-yn-1-yl)-phenanthrene (**R3**) was synthesized by Sonogashira coupling of 9-ethynylphenanthrene with vinyl bromide (**Scheme 2**). $Pd(PPh_3)_4$ (5.8 mg, 0.005 mmol) and Cu(I)I (3.8 mg, 0.02 mmol) were placed in the flame-dried flask under N_2 at 0 ^oC (ice-bath). Then Et_2NH (0.65 mL, 460 mg, 6.29 mmol) and vinyl bromide (1.0 M in THF; 0.65 mL, 0.65 mmol) were added. Next, commercially available 9-ethynylphenanthrene (101.1 mg, 0.5 mmol) dissolved in dry THF (1 mL) was added slowly via a syringe pump (over 3 h) and the resulting mixture was allowed to warm up to ambient temperature (30 min) and was stirred for another 2 h. Volatiles were evaporated and the residue was dissolved in EtOAc and filtered. The filtrate was collected with the solvent evaporated. The residue was column chromatographed (*n*-hexane) to give **R3** (50 mg, 44%) as white powder: ^1H NMR ($CDCl_3$, 400 MHz) δ 5.65 (dd, J = 11.2, 2.0 Hz, 1H), 5.89 (dd, J = 17.6, 2.0 Hz, 1H), 6.20 (dd, J = 17.2, 11.2 Hz, 1H), 7.58-7.62 (m, 1H), 7.65-7.73 (m, 3H), 7.85 (d, J = 7.6 Hz, 1H), 8.01 (s, 1H), 8.42-8.45 (m, 1H), 8.65-8.70 (m, 2H); ^{13}C NMR ($CDCl_3$, 100.6 MHz) δ 88.39, 92.75, 117.42, 117.47, 119.70, 122.66, 122.82, 122.98, 127.14, 127.39, 127.70, 128.74, 130.23, 130.45, 131.21, 131.37, 132.05, 132.09.

It is noteworthy that regular coupling conditions, as reported recently for the synthesis of the analogous (but-3-en-1-yn-1-yl)-benzene,[7] yielded mainly dimerization and/or polymerization products of 9-ethynylphenanthrene.

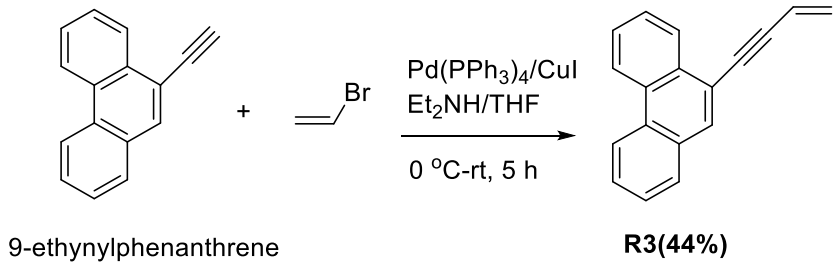

Scheme 2. Synthesis of 9-(but-3-en-1-yn-1-yl)-phenanthrene (**R3**).

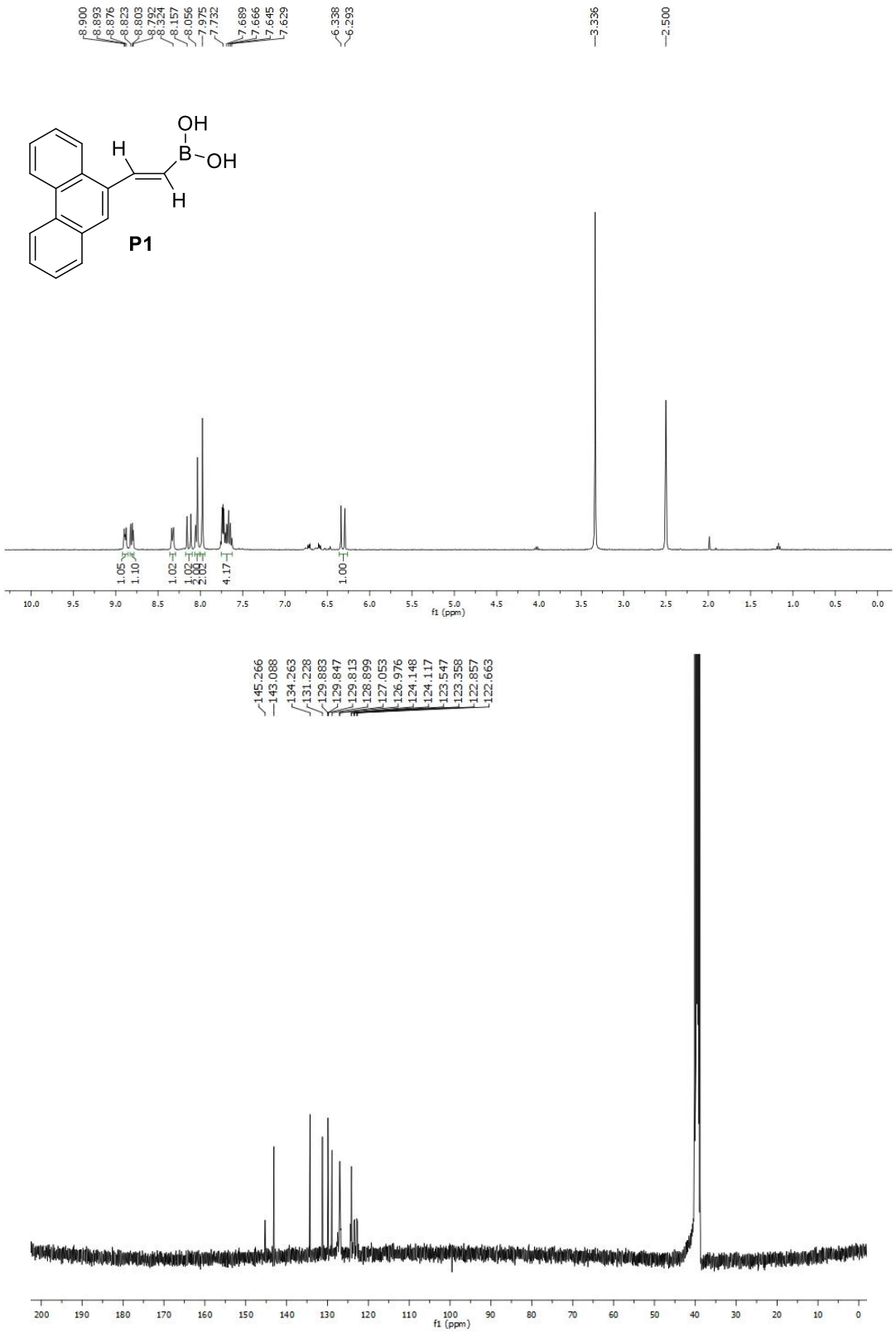

Figure S5: ^{1}H NMR and ^{13}C NMR spectra of compound **P1** in DMSO-d_6.

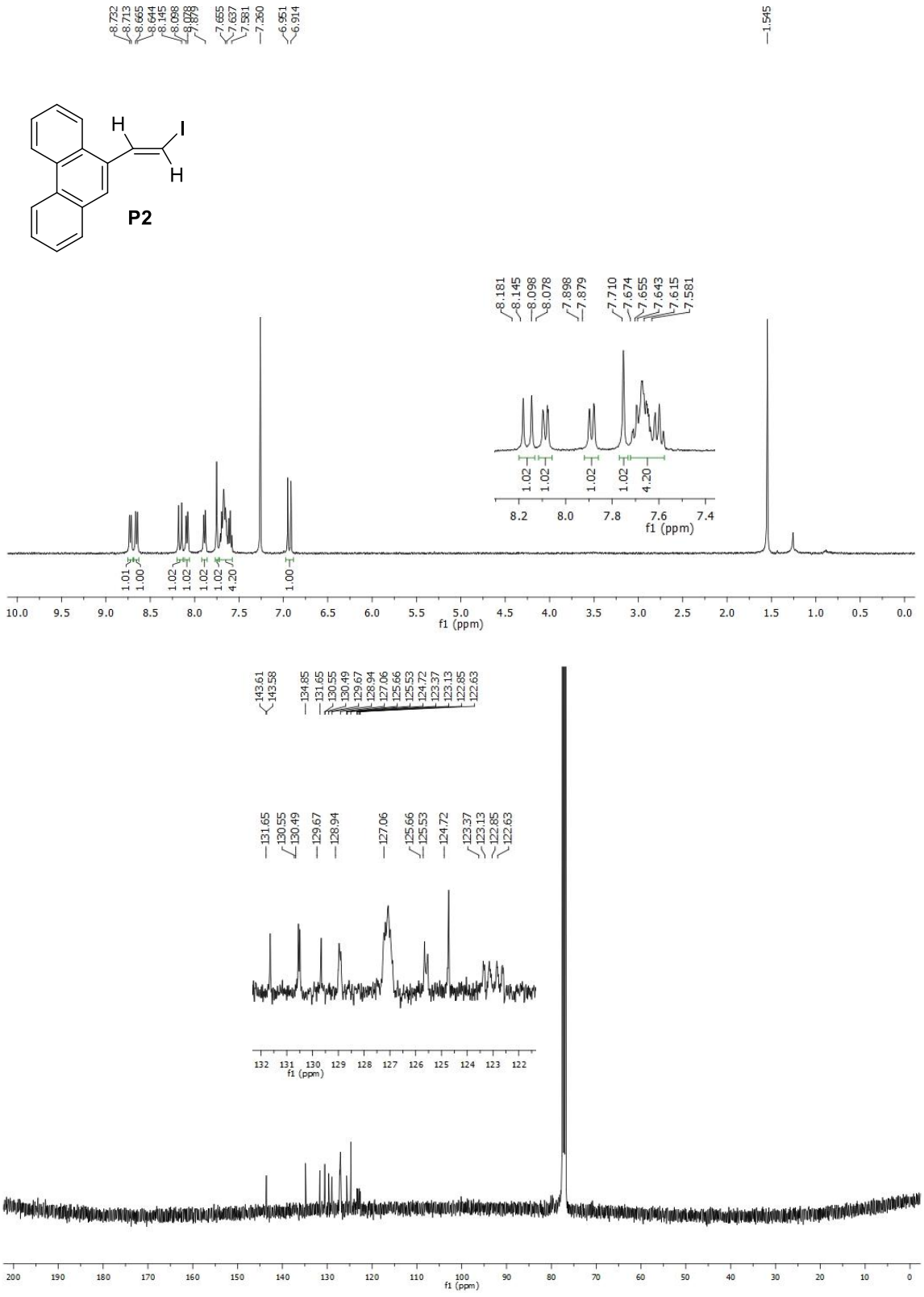

Figure S6: ^{1}H NMR and ^{13}C NMR spectra of compound **P2** in $CDCl_3$.

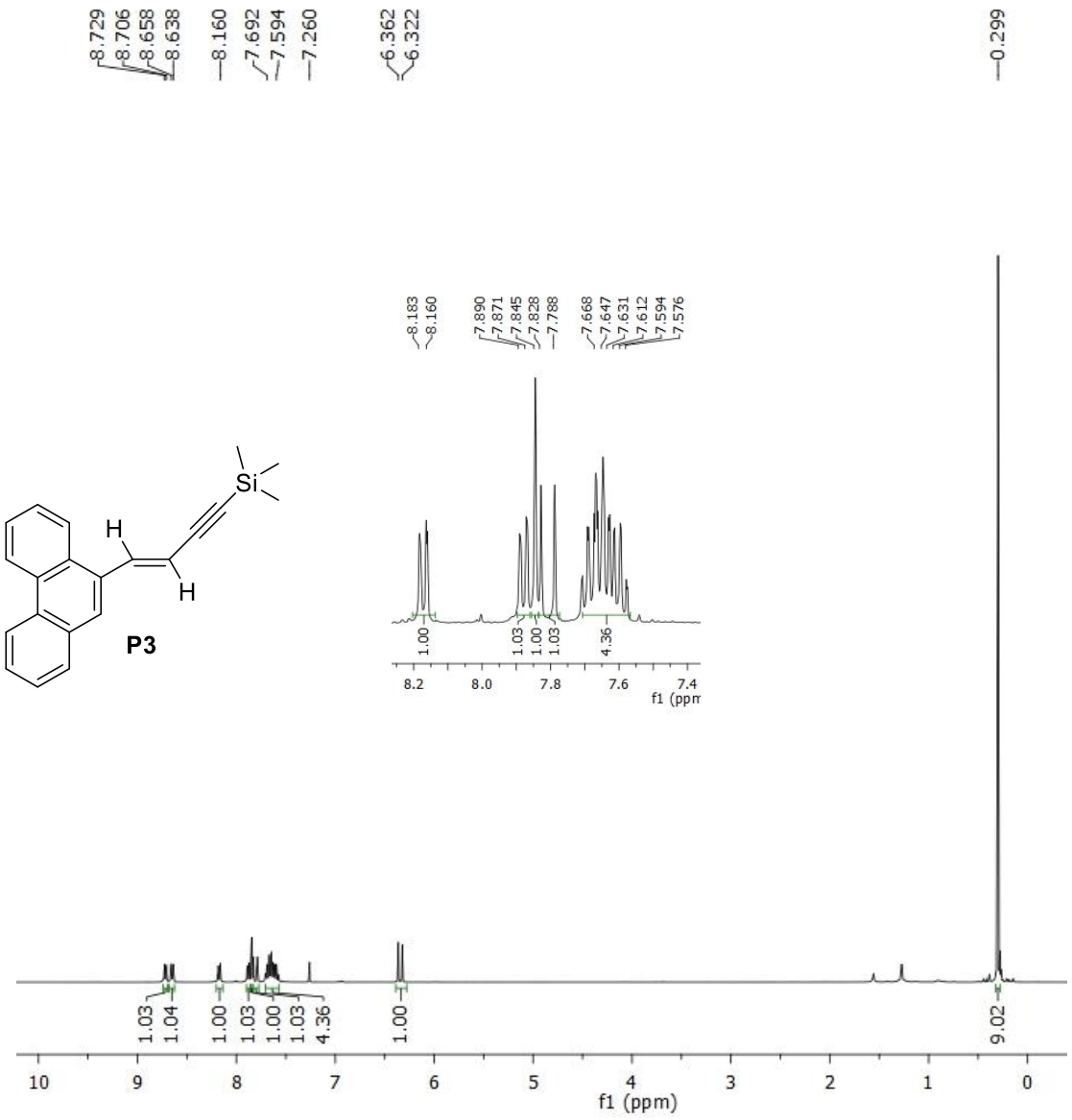

Figure S7: ^{1}H NMR spectrum of compound **P3** in $CDCl_3$.

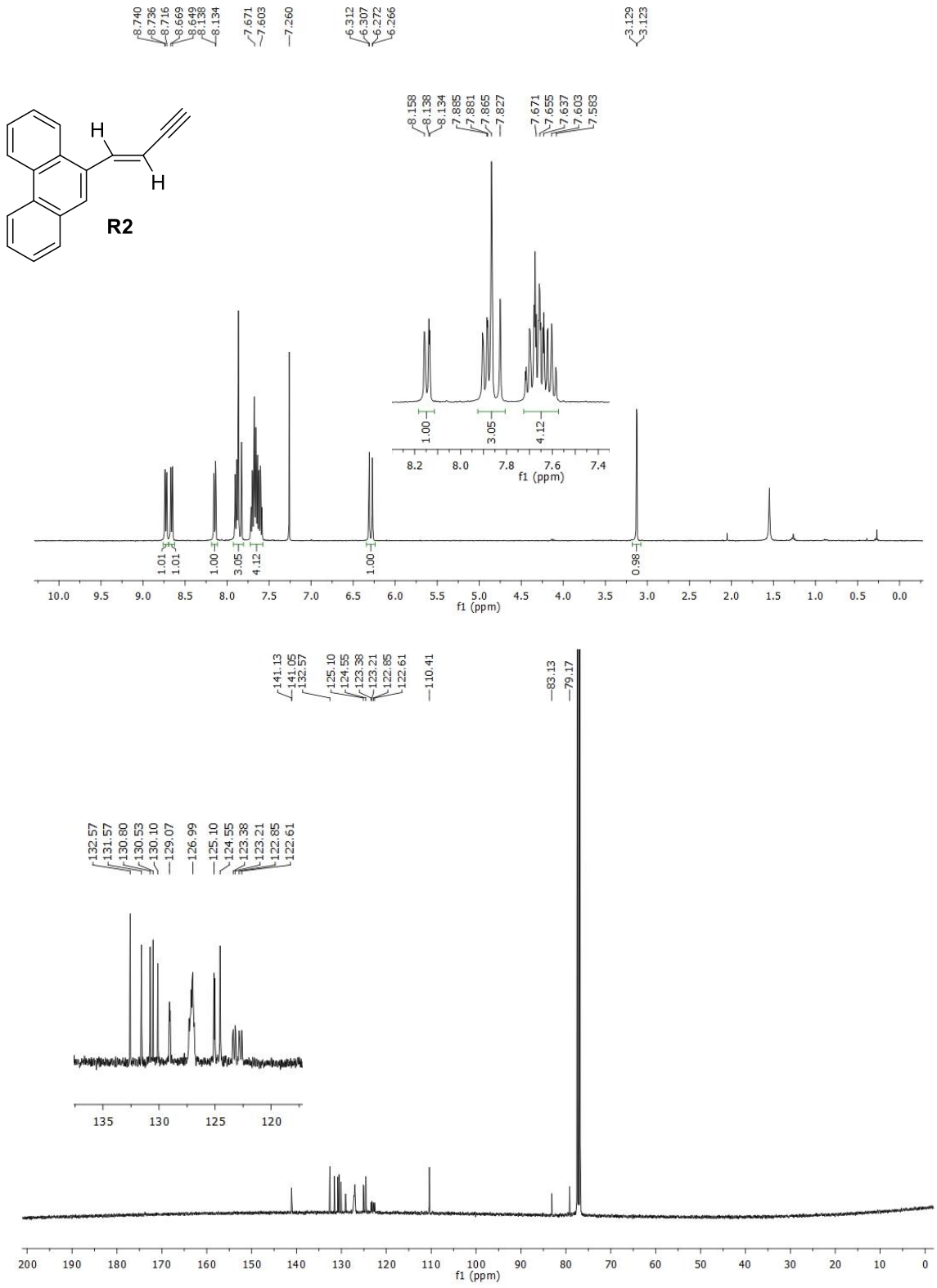

Figure S8: ^{1}H NMR and ^{13}C NMR spectra of compound **R2** in $CDCl_3$.

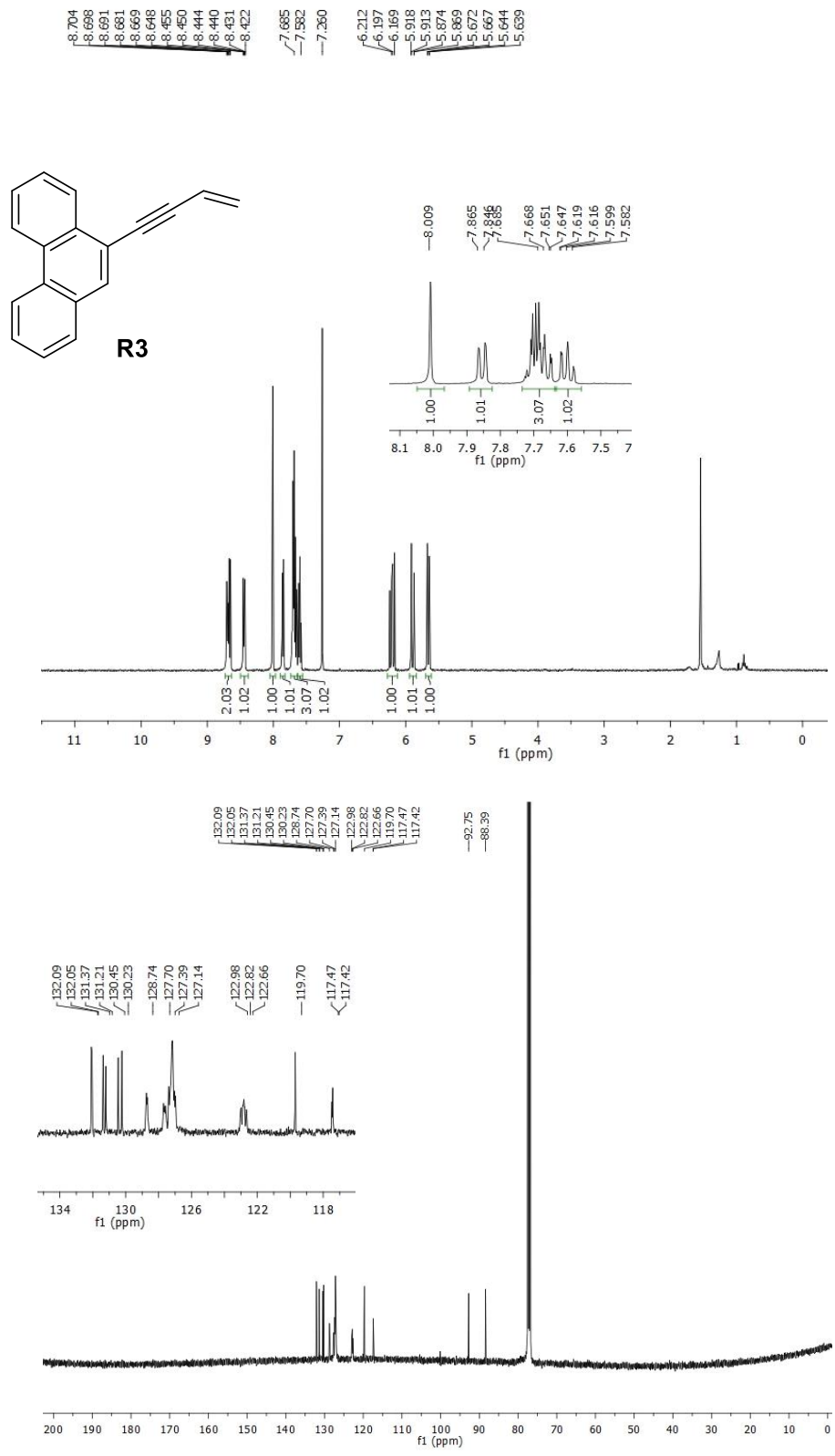

Figure S9: ^{1}H NMR and ^{13}C NMR spectra of compound **R3** in $CDCl_3$.

References:

[1] L. Zhao, R. I. Kaiser, B. Xu, U. Ablikim, M. Ahmed, D. Joshi, G. Veber, F. R. Fischer, A. M. Mebel, *Nat. Astron.* **2018**, *2*, 413-419.

[2] M. Dewar, D. Goodman, *J. Chem. Soc. Faraday Trans.* **1972**, *68*, 1784-1788.

[3] K. O. Johansson, M. F. Campbell, P. Elvati, P. E. Schrader, J. Zador, N. K. Richards-Henderson, K. R. Wilson, A. Violi, H. A. Michelsen, *J. Phys. Chem. A* **2017**, *121*, 4447-4454.

[4] W. Schmidt, *J. Chem. Phys.* **1977**, *66*, 828-845.

[5] H. C. Brown, T. Hamaoka, N. Ravindran, *J. Am. Chem. Soc.* **1973**, *95*, 5786-5788.

[6] M. R. Uehling, R. P. Rucker, G. Lalic, *J. Am. Chem. Soc.* **2014**, *136*, 8799-8803.

[7] L. Zhao, R. I. Kaiser, B. Xu, U. Ablikim, M. Ahmed, M. V. Zagidullin, V. N. Azyazov, A. H. Howlader, S. F. Wnuk, A. M. Mebel, *J. Phys. Chem. Lett.* **2018**, *9*, 2620-2626.